

## **GROUND RESONANCE TEST AND AEROELASTIC MODEL VALIDATION OF AN INNOVATIVE REGIONAL AIRCRAFT FITTED WITH INNOVATIVE WING TIP (IWT) AND ADAPTIVE MORPHING WINGLET (AMW)**

**S. Nocerino<sup>1</sup>, S. Di Cristofaro<sup>1</sup>, B. De Maio<sup>1</sup>, N. Calvi<sup>2</sup>, E. Orazi<sup>2</sup>**

<sup>1</sup> Leonardo Aircraft Division Large Structures Laboratories  
Viale dell'Aeronautica, snc, 80038 Pomigliano d'Arco, Naples, Italy  
[salvatore.nocerino@leonardo.com](mailto:salvatore.nocerino@leonardo.com)  
[salvatore.dicristofaro@leonardo.com](mailto:salvatore.dicristofaro@leonardo.com)  
[biagio.demaio@leonardo.com](mailto:biagio.demaio@leonardo.com)

<sup>2</sup> Leonardo Aircraft Division Aeroelasticity Engineering  
Corso Francia 426, 10146 Turin, Italy  
[natale.calvi@leonardo.com](mailto:natale.calvi@leonardo.com)  
[edoardo.orazi@leonardo.com](mailto:edoardo.orazi@leonardo.com)

**Keywords:** Ground Resonance Testing, normal mode testing, modal analysis, aeroelastic model optimization, Aeroelasticity, Adaptive Structures

**Abstract:** These last years, many economic and financial efforts have been made by the European Commission in order to encourage more and more the manufacturing of Innovative Regional Aircraft all over the world.

Leonardo is leading several research project launched in the CLEAN SKY 2 (CS2) field. The major challenges here presented are the design and the related aeroelastic qualification of newer systems aimed at in-flight load control & alleviation, such as the innovative wingtips (IWT) and the adaptive morphing winglets (AMW) that have been tested on-ground and the IWT also in-flight, installed on the CS2 FTB#1 (Flight Test Bed) demonstrator, used to achieve the TRL6.

The first flight in configuration FTB#1+IWT has been performed in 12/02/2024.

On the roadmaps that bring to the permit to fly, aeroelastic clearances must be provided by theoretical analysis using a mathematical model validated by Ground Resonance Test (GRT) data. GRT is always focused to measurement of each resonance structural mode in terms of frequency, structural damping and modal shape; it has always been a critical issue causing by both significant delay about the aircraft preparation for the flights and how much time is allowed for testing. All this hardly ever fit to the massive time frame asked for GRT.

This paper describes the GRT performed on the CS2 FTB#1 demonstrator and the Leonardo Aircraft Division's validation methods applicable for the matching between experimental data and theoretical ones coming from the aeroelastic models. The validated models are used to provide initial flight clearances as concerns the aeroelastic aspects.

## 1 INTRODUCTION

In this paper there will be dealt with all characteristic steps for the ground test campaign running, data post-processing and finally test data correlation with aeroelastic model used to provide the flight clearances and the related permit to fly tests aimed at reaching the TRL6 of the studied technologies.

This Project has received funding from the Clean Sky 2 Joint Undertaking under the European Union's Horizon 2020 research and innovation programme under Grant Agreement n° 945548.

A Ground Resonance Testing (GRT) is the most used method for the experimental performing of aircraft modal measurements and analysis. All GRT concepts are used to be associated to the natural deformation that a full-scale aircraft structure generally takes when excited by external forces. The expected GRT results are inherent to the dynamic response of structure through modal parameter extraction such as natural frequencies, modal damping factors and modal shapes over a specified frequency bandwidth.

Starting off the needed test setup configuration, then moving on to the effective test procedure, next turning to most common algorithms used for the test data post-processing, and at last concluding with innovative Genetic Algorithm aimed at the matching between theoretical and experimental modal data for dynamic model updating in use for aeroelastic assessments and flight clearances provision.

The final goal of GRT is nowadays a very charming chance for getting aeroelastic predictions in a short time with validated models, in order to approach the first flight and the speed expansions with adequate safety margins and without significant effects on the current schedule and on the other schedules. Since focused on the measurement of structural natural resonance characteristics as frequency, damping and modal shape, the term GRT is here considered rather than the general GVT that is more appropriate for general vibration measurements.

On the A/C C-27J FTB#1 two advanced wing tip devices, the AMW and the IWT, fitted with particular control surfaces can be installed. The movement of these particular control surfaces are able to regulate in real time the aerodynamic load distribution with the aim of optimizing the A/C attitude, the performances and the fuel consumption during the flight, with a significant contribute to the environment impact.

The in-flight tests performed by the C-27J FTB#1 in Torino-Caselle on February 2024 have completed the technological demonstration REG IADP concluding a European developing that lasted about ten years.

In this paper it shall be mentioned all technical and operative methods and approaches to meet this commitment.

## 2 ACRONYMS AND SYMBOLS

<b>A/C</b>	Aircraft
<b>AMW</b>	Adaptive Morphing Winglet
<b>CFD</b>	Computational Fluid Dynamics
<b>CIRA</b>	Centro Italiano Ricerche Aerospaziali
<b>CPM</b>	Complex Power Method
<b>CS2</b>	Clean Sky 2
<b>DLM</b>	Doublet Lattice Method
<b>DMI</b>	Direct Matrix Input
<b>DOE</b>	Design Of Experiments
<b>DOF</b>	Degree of Freedom
<b>EDM</b>	Exponential Decay Methods
<b>FAM</b>	Force Appropriation Method
<b>FEA</b>	Finite Element Analysis
<b>FEM</b>	Finite Element Method
<b>FQM</b>	Force Quadrature Method
<b>FRF</b>	Frequency Response Function
<b>FTB</b>	Flight Test Bed
<b>GA</b>	Genetic Algorithm
<b>GRT</b>	Ground Resonance Test
<b>GVT</b>	Ground Vibration Test
<b>IPC</b>	Integrated Circuit Piezoelectric
<b>IWT</b>	Innovative Wing Tip
<b>LAD</b>	Leonardo Aircraft Division
<b>LCO</b>	Limit Cycle Oscillation
<b>LH</b>	Left Hand
<b>MAC</b>	Modal Assurance Criterion
<b>MIMO</b>	Multi Input Multi Output
<b>MIF</b>	Modal Indicator Factor
<b>MNM</b>	MIMO Normal Mode
<b>MPC</b>	Modal Phase Collinearity
<b>MPD</b>	Mean Phase Deviation
<b>NM</b>	Normal Mode
<b>PI</b>	Phase Index
<b>PRM</b>	Phase Resonance Method
<b>PSM</b>	Phase Separation Method
<b>Polimi</b>	Politecnico di Milano
<b>REG IADP</b>	REGional Integrated Aircraft Demonstration Platform
<b>RH</b>	Right Hand
<b>TRL</b>	Technology Readiness Level
<b>SOF</b>	Single Degree of Freedom
$\xi$	Damping Coefficient
$\mu$	Generalized Mass
$\omega$	Natural Frequency
$\phi$	Mode Shape

### 3 DESCRIPTION OF AIRCRAFT AND WING TIP DEVICES

The A/C used as in-flight technological demonstrator (FTB#1) to achieve the TRL6 for the Clean Sky 2 European program is the LAD prototype C-27J Spartan.

This Project has received funding from the Clean Sky 2 Joint Undertaking under the European Union's Horizon 2020 research and innovation programme under Grant Agreement n° 945548.

The C-27J Spartan is a medium-class tactical transport A/C fitted with Rolls Royce AE 2100-D2A systems and engines 4,637 SHP.

The wing tips of the FTB#1 have been modified on in order to install two innovative devices: the AMW and the IWT.

The AMW and the IWT are fitted with particular control surfaces. The movement of these particular control surfaces are able to regulate in real time the aerodynamic load distribution with the aim of optimizing the A/C attitude, the performances and the fuel consumption (lower emissions) during the flight, with a significant contribute to the environment impact.

The Figure 1 shows the A/C fitted with IWT during the take-off of the first flight carried out in Turin on February 2024 and Figure 2 the A/C fitted with AMW during the GRT campaign.



*Figure 1 – FTB#1 fitted with IWT*



*Figure 2 – FTB#1 fitted with AMW (right wing)*

### **3.1 Adaptive Morphing Winglet AMW and Nastran Model**

The following Figure 3 reports the adaptive winglet AMW installed on the right wing tip during the related GRT tests.

The vertical height of the AMW is about 1 m and it is fitted with two “fingered” control flaps on trailing edge (green surfaces); an inner and smaller spanwise flap (near to the wing surface) and an outer and larger spanwise flap. Both flaps have the same chord and their rotations, comprise between  $-15^\circ$  and  $+5^\circ$  are self-regulating based on appropriate control laws aimed at loads control.

The AMW aims to enhance the A/C aerodynamic efficiency in off-design flight conditions by providing optimal winglet aero-shapes by the finger’s positions (Figure 4) for optimal wing lift distribution, throughout the A/C flight envelope and to reduce wing loads at critical flight points with the aim of alleviating the loads.

The main improvements that should be provided by AMW are a reduced Drag (approximately 2%) for the design mission with benefits on noise and fuel consumption, reducing thus emissions of  $\text{CO}_2$  and  $\text{NO}_x$ .

The Nastran model of the AMW device has been designed and provided by CIRA, developed in the framework of Clean Sky 2 project. The AMW model has been connected on the tip of the wing beam of the FTB#1 model as shown in Figure 5.

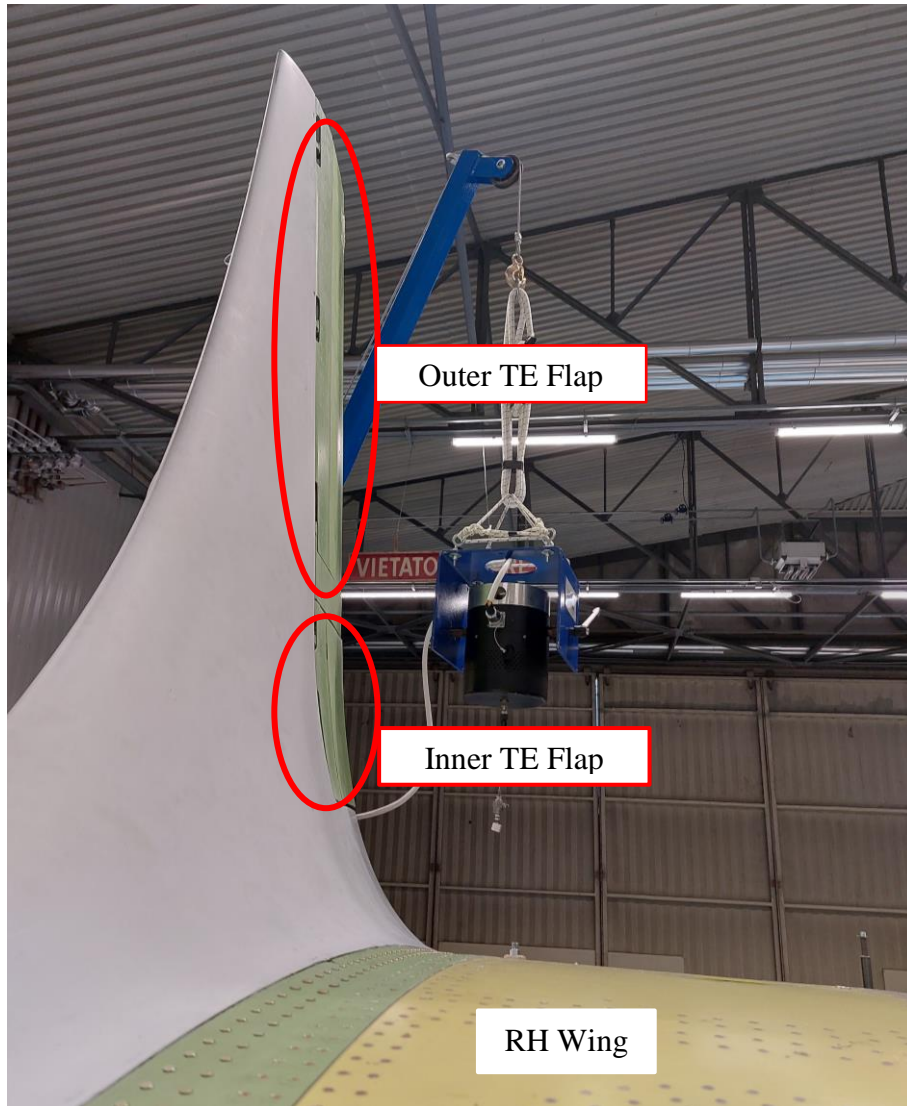


Figure 3 – AMW (right wing)

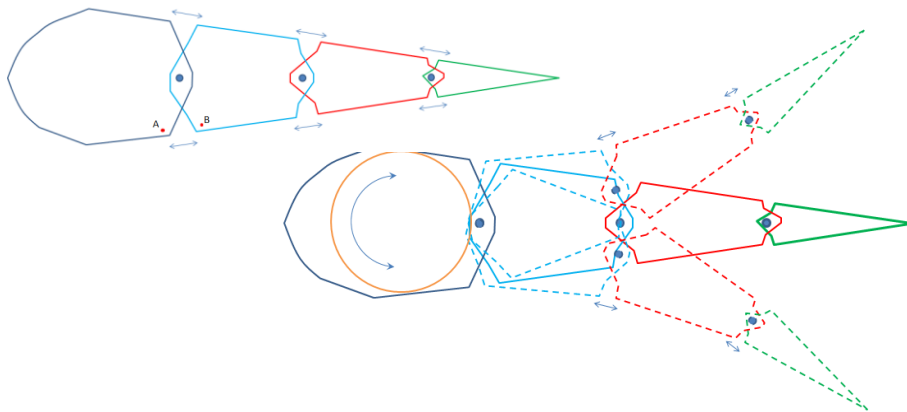


Figure 4 – AMW Flap Finger's scheme

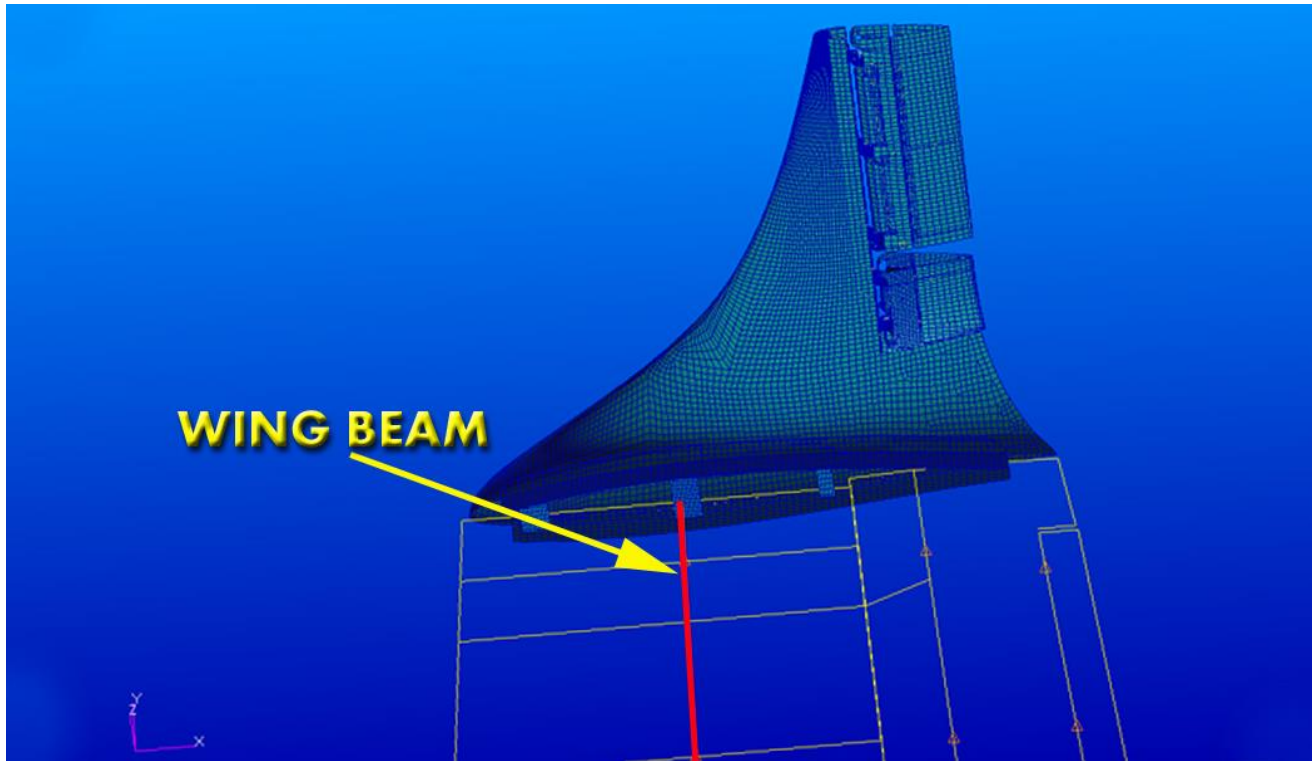


Figure 5 – AMW on Right Wing Tip of FTB#1 (Nastran model)

### 3.2 Innovative Wing Tip IWT and Nastran Model

The following Figure 6 shows the innovative wing tip IWT installed on the right wing tip of FTB#1. Looking at the figure it can be seen that a movable flap is installed on the IWT trailing edge. The rotations of the right and left flaps, between  $\pm 15^\circ$ , are self-regulating based on appropriate control laws aimed at loads alleviation.

The aim of IWT is to reduce, by proper rotations of IWT's flaps, the peaks generated by manoeuvre and gust loads and to contribute to the flight performance improvements during climb. Potentially, structural weight would be saved with an impact on fuel consumption reduction, and fatigue life could be extended due to the alleviation of peak loads.

The Nastran model of the IWT has been designed and provided by PoliMi, developed in the framework of Clean Sky 2 project. The IWT model has been then installed on the tip of the wing beam of the FTB#1 model as shown in Figure 7.

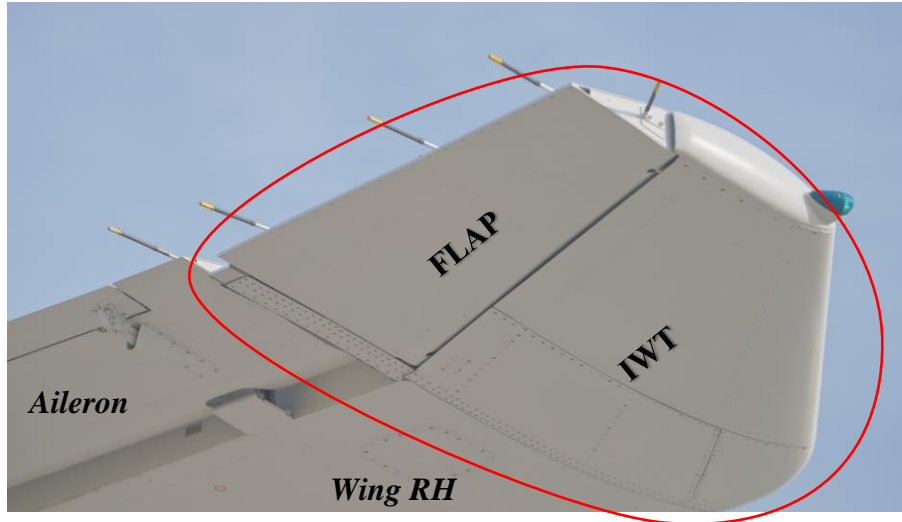


Figure 6 – IWT (right wing)

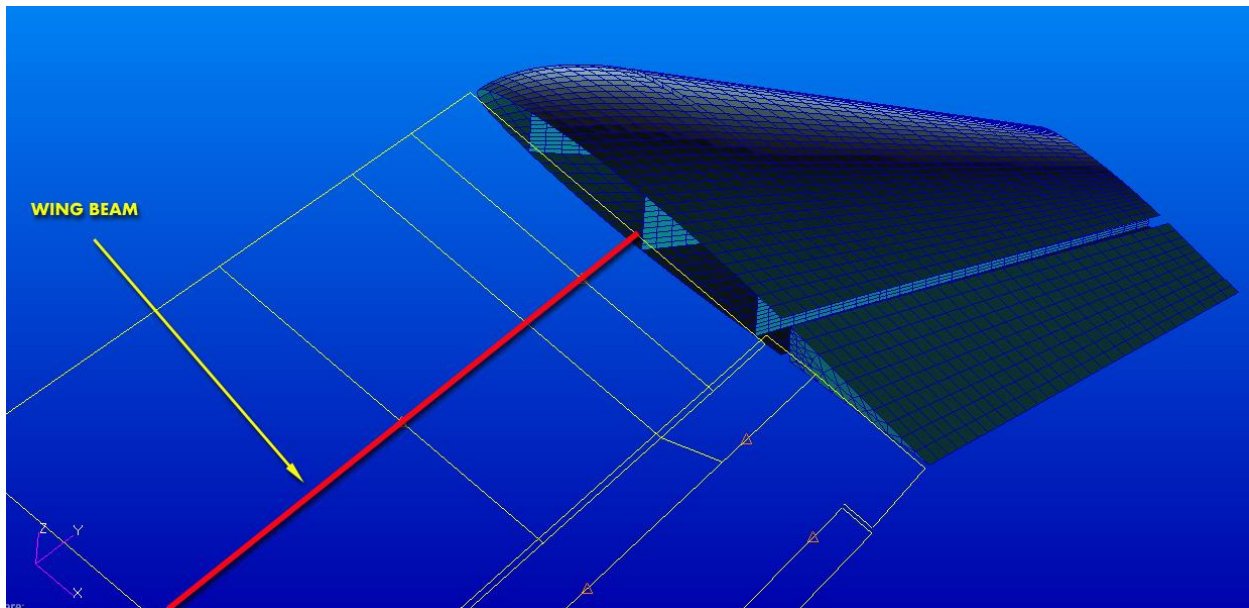


Figure 7 – IWT on Right Wing Tip of FTB#1 (Nastran model)

## 4 TEST SETUP

### 4.1 Soft suspending system

Before starting with a GRT, a plenty of attention by engineers is dedicated to the selection of an adequate method for the A/C suspending to decouple the A/C from the on-ground effects (landing gear and tyres). The method applied is generally strongly dependent on the A/C proprieties. The



best practical solutions consisting in free-supports that can approximate a free-free vibration condition.

The GRT setup realized for this topic is shown in Figure 8. In this context, it has been used a soft suspending system consisting mainly in three pneumatic supports. It is used to sustain an A/C by means of its hoisting points. On this A/C there are two hoisting points under the wings and one under the fuselage-nose. Thus, two cylindrical units equipped by screw jack system and levelling valves have been placed under the wings by means of mobile tripods four meters high. A single device, consisting in two separated beams (having a star-form) isolated each other by six AirRide units, has been disposed forward. Fitting plates have been built to host the A/C by means of a ball-sleeve joints.

The benefits coming from the using of this suspending system is the complete decoupling between the rigid body modes (due mainly to the supports) and first flexible A/C modes, allowing rigid body frequencies below 1 Hz.



Figure 8 – GRT soft suspending system setup

In basis of the amount of expected A/C weight present on each support it can be evaluated the air pressure of pneumatic supports and relevant frequencies of A/C rigid mode. The single backward unit has been designed with natural frequencies no greater than 0,8 Hz. Besides, for the forward unit the natural frequencies are given by AirRide characteristics eventually. Considering that for this test article the first elastic modes appear above the 2.5 Hz, the rigid modes have been completely decoupled by flexible ones.

#### 4.2 Driving and Response point

The core of GRT is the FRF measurements. From the post-processing of them, it is possible to achieve the modal characteristics of the complete aircraft and its control surfaces, in detail:

- Resonance frequencies  $\omega_n$ ,
- Mode shapes  $\varphi_n$ ,
- Generalized masses  $\mu_n$  and damping ratios  $\xi_n$ ,
- Structural non-linear behaviour.

The frequency range of the GRT has been defined with the aim to identify all modes of interest, from rigid body modes to the last A/C flexible mode coming from in the aeroelastic range of investigation.

A FRF is always defined as a ratio of output signal (Response Point) to the input signal (Excitation or Driving Point) in frequency domain.

According to modern test methods, a set of Response Point should be used to measure all important modes seen in the FEA. To optimize the number and location of Response Point, some recommendations are supposed to be taken. Firstly, to avoid that accelerometer acting along the same direction are placed close to each other. Then it is always advised to choose the best location to extract the required mode shapes, i.e., all those A/C points that have proved higher responses.

LAD has developed user-friendly routines working in Matlab environment that able to optimize the number of Response Points.

Because the FTB#1 A/C derives from the C-27J, whose normal modes are well known, up to 60 accelerometers have been considered enough for modal acquisition with IWT or AMW installed on the wing tips. The accelerometer locations for the GRT in question are shown in Figure 9, Figure 10 and Figure 11.

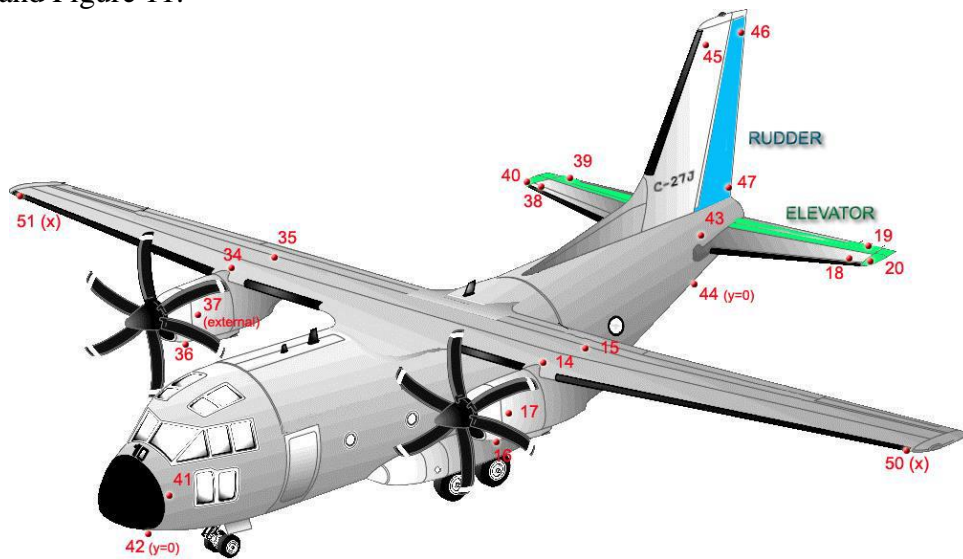


Figure 9 – Accelerometer Map – A/C Layout

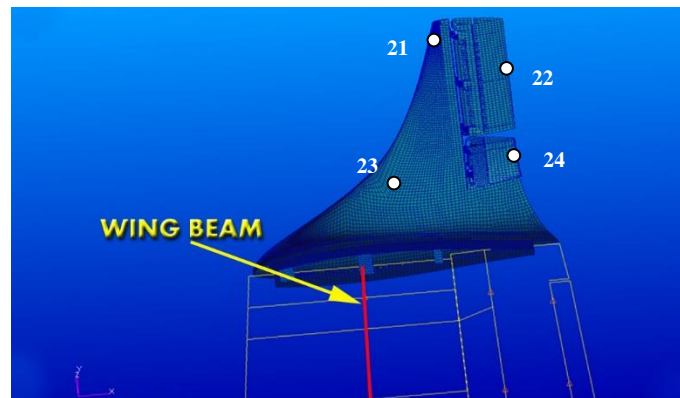


Figure 10 – Accelerometers Map – AMW Layout (Right Wing Tip)

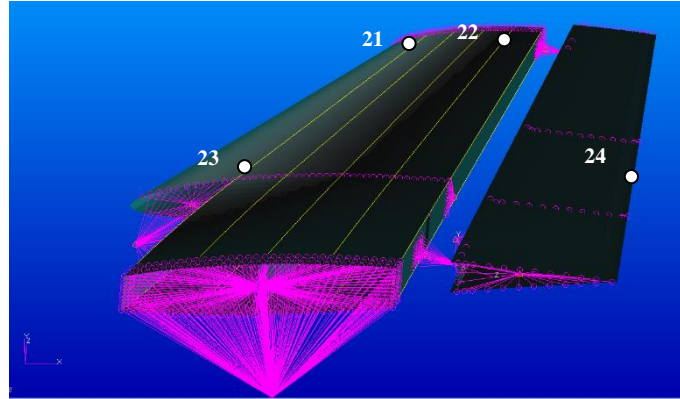


Figure 11 – Accelerometers Map – IWT Layout (Right Wing Tip)

Excitation is the method of transferring the energy to a structure to excite by means of input force. It is important to not excite the structure by its nodal points (zero modal deflection during vibration) where the external energy cannot be transferred to the structure. Another useful consideration is to excite through “hard point” for example an intersection of a spar and rib, where there is enough structural stiffness to excite the normal modes. Sometimes, it is convenient to apply an excitation force at an inclination to the plane of application of force to excite simultaneously more modes like the bending modes and torsion modes.

The best method for searching modal frequencies in a structure is to take measurements (force and acceleration) at several locations to identify each mode and the respective natural frequency. A thorough knowledge of the FEA allows to select the best excitation point locations well before GRT is performed.

Generally, the best practice is to choose as excitation point at any points characterized by a high amplitude of the A/C response and they are settled on:

- A/C surface tip like wing, stab, fin,
- A/C fuselage nose, engines, and stores (if any),
- A/C control surface like ailerons, elevators, and rudder.

### 4.3 Equipment

GRT always requires a huge number of accelerometers distributed on large A/C structure, making very hard the management of cables for sensor connections. As well as sensor increases, a lot of cables are supposed to be handled and built.

For a long time, LAD’s Laboratory has adopted a different methodology to reduce the amount of length and number of passages around the A/C of the cabling. The entire A/C structure is divided in more sections (for example left and right wing, tail, nose, and rear fuselage and so on), in each of them, all present sensor cables are led to a unique and centralized point. Then all data present in each section travels on an internal reflected optical memory and all available for the central data measurement and control system.

In this scenario 60 ICP accelerometers have been installed over the entire structure of A/C by well-trained personnel of Large Structures Laboratories. In Figure 12 some examples of accelerometers installation are depicted. Many brands of accelerometers (PCB, Kistler, B&K) can be used and with different measurement.

The data acquisition and control system are formed by three acquisition frontends: two units have been positioned under the wing surfaces and they have been laid on the tripod trays of the suspending system; another one has been positioned on a scaffolder situated under A/C tail.

In this case, the length of sensor cable has been approximatively reduced to 280 m with a saving of 54% with respect to initial cable distribution solution having a unique central point to lead any sensor cables.



*Figure 12 – Examples of accelerometers installation*

In this scenario, various excitation locations have used to properly excite all modes of interest of the A/C and of its innovative devices. Essentially, a total of two different type of shakers (PCB and TIRA) have been used. It is a widespread common practice to have available a plan to quickly move one point of excitation on the next ones without long break.

Very performant shakers are nowadays available in LAD. They are firstly very light and so easy to move on different excitation points. Then they can generate relevant vibrations into the structure and come up with force up to 220 Npk/140 Nrms with their cooling system and the halves without them though. They must be powered by advanced power amplifiers by 500W of a maximum power.

Shakers are usually suspended by mobile and adaptable mechanical structures. In Figure 13 typical shaker installation used in GRT have been shown. At high height such as rudder or fin tip, alternative installation solutions have been studied and, in these circumstances, it is better to mount shaker on either crane or ad-hoc and sophisticated structure. The excitation forces have been measured by force cells installed on the rod-end of any single shaker.

In GRT, LAD Large Structures Laboratories nowadays uses a data acquisition and control system based by the combination of more than one Siemens Scadas III frontends and controlled by Simcenter TestLab™ software. In this paper application, a distributed data acquisition system built by three frontends has been placed around A/C to route the analogue signals. These frontends have been daisy-chained by using three fiberoptic cables long 50 meters each one and operate as a single monobloc system with perfect synchronization between all included channels. The acquisition modules inside Scadas frontends have a high-pass filter with cut-off frequency of 0.05Hz. This very low high pass filter makes possible to identify even the low rigid body modes of an aircraft on pneumatic suspensions, so that the boundary conditions can be accurately determined.



*Figure 13 – Shaker installation*

## 5 GRT METHODS

The classical excitation signals used during a GRT are known as random (burst, periodic and so on) and swept sine signals with more than one activated exciter to take full advantage from multi-shaker excitation in terms of both available energies to excite properly the structure and time-consumption saving.

For modal identification of A/C structure in GRT, nowadays there are two available methods, and these ones can be mainly classified into two groups, namely phase resonance (PRM) and phase separation method (PSM). PSM appears to be the most privileged all over the world because many modes are excited in a single excitation run that are separated mathematically afterwards. These methods are usually based on user-defined swept sine excitation signals over frequency bandwidth and the using of dedicated signal processing algorithms.

Different excitation force levels have also been shown to detect the non-linear behaviour of the structure.

After applying the PSM, the PRM otherwise known as MNM testing is usually performed by LAD. Here, the structure is forced to act as a SOF system and the vibration response will contain just right the mode of interest.

Advantages of PRM are the real modes of corresponding structure are directly measured, then the eigenvectors are excited at high energy levels, and lastly the very closed modes to each other can

be separated with linearity test easily to be performed. The main disadvantage of the PRM is that it is time consuming, but LAD has already been learning by its background.

Various input signals and used methods in GRT are reported in Figure 14.

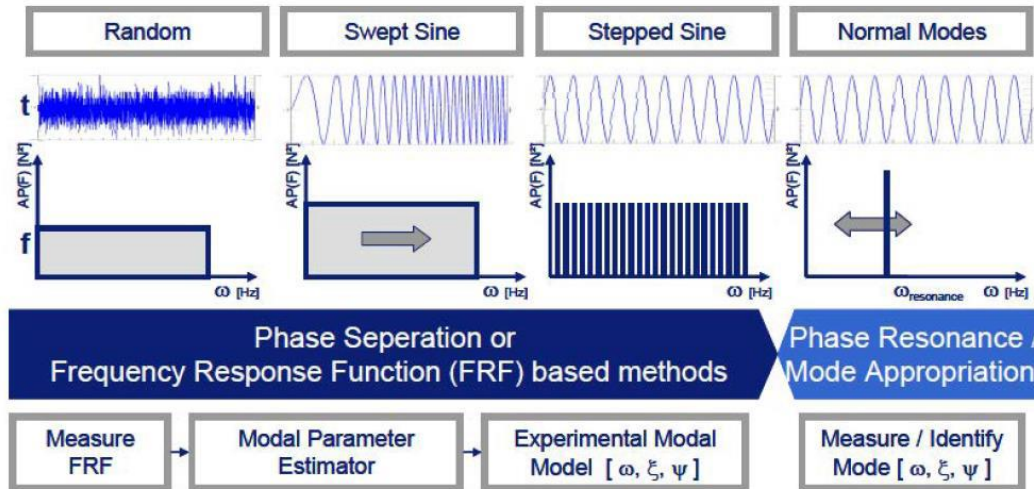


Figure 14 – GRT methods

## 5.1 Phase Separating Method

The PSM uses single or multiple broadband excitation signals to excite the structure so that all desired modes are excited simultaneously. For these purposes, the structure is usually subjected to different excitations regarding to amplitude level, location, and direction.

Generally, LDO uses random excitations for the test setup validation first and then to achieve a quick overview of the A/C structural dynamic behaviour. It is always used to start with very low excitation levels of input energy and then increasing them step-by-step upon to approach certain levels in such a way to pull the expected results out. Once that a quick overview has been obtained, tailored swept sine runs with well-defined force level are performing. MIMO sine stepped and swept testing tools present inside of TestLab<sup>TM</sup> package is employed for these purposes. Even if for time-consuming constrains not more two exciters can be simultaneously used during the sine with respect to random excitations.

Even though often to make real effort to shorten the GRT schedule, many multi-shakers random excitations are used at the same time. By the Leonardo practical expertise, multi-input excitations having high levels are useful to quickly extract all modes at high frequency, where nearly the whole amount of excitation energy for single shaker tends to be uniformly distributed into the frequency range. Whereas at low frequency, the requested energy to excite all proper modes could be very hard to handle in a proper way. In these circumstances, the frequency bandwidth is supposed to be reduced to a few Hertz and the excitation level on the single driving point might be set properly to acquire the mode of interest with a good resolution. This case usually happens for the first wing modes where a huge amount of energy is needed to excite them.

Another useful consideration for GRT is to apply localized swept sine runs having also different force levels only to that frequency range. There where they already know in advance that reside some modes of interest. This strategy is sometimes used to identify non-linear behaviour of A/C modes with respect to the input force level increasing. The mode is considered linear when the resonance frequency trend is asymptotic with respect to the increment of the force levels.

Back in the days, from the measure of FRFs many curve fitting parameter algorithms have been developed in time and frequency domain for estimation of modal parameters. In each of them, the FRFs have been dealt with rational fraction functions, and an error function has been established in a way that the resulting system of equations were linear. Because the resulting linear system of equations involves ill-conditioned matrices, the gradient method has been used to minimize the error functions. After obtaining the coefficients of rational fractions the modal parameters can be estimated. One of the most popular modal parameter estimators used by Leonardo, is POLYMAX (a Siemens solver), it plays an important role in reducing analysis time and providing the modal parameters.

## 5.2 Phase Resonance Method

As know the equation of motion of a system with N degrees of freedom (DOF) can be written as follows:

$$[M]\{\ddot{x}\} + [C]\{\dot{x}\} + [K]\{x\} = \{F\} \quad \text{Eq. [1]}$$

where [M], [C] and [K] matrices represent respectively the mass, damping and stiffness;  $x$  is the displacement,  $\dot{x}$  the velocity and  $\ddot{x}$  the acceleration.

For most practical analysis, however, a proportional damping behaviour can be assumed resulting in a diagonal damping matrix. In general, these matrices have nonzero off-diagonal elements so that the N equations are coupled.

The purpose of a PRM is to uncouple these equations. This is accomplished by identifying the mode shapes. Let assume the mode shapes,  $\{\varphi_n\}$ , are real values. Any arbitrary pattern of motion,  $\{x\}$  is a linear combination of N mode shapes  $\{\varphi_n\}$ , where the weighting coefficients of this summation are provided by the modal participation vector,  $\{q\}$

$$\{x\} = [\{\varphi_1\} \dots \{\varphi_n\} \dots \{\varphi_N\}] \{q\} = [\varphi] \{q\} \quad \text{Eq. [2]}$$

The NM solution vectors have an important mathematical property termed "generalized orthogonality" with respect to mass, stiffness, and damping matrices. This property can be used to diagonalize all three matrices when applied as a similarity transformation. Once the transformation is performed upon diagonalization mass, stiffness, and damping matrices, we have

$$[\varphi]^T [M] [\varphi] \{q''\} + [\varphi]^T [C] [\varphi] \{q'\} + [\varphi]^T [K] [\varphi] \{q\} = [\varphi]^T \{F\} \quad \text{Eq. [3]}$$

If mass normalization of mode shapes is done, the above equation can be rewritten as follows:

$$\text{diag}(1) \{q''\} + \text{diag}(2\xi_n \omega_n) \{q'\} + \text{diag}(\omega_n^2) \{q\} = [\varphi]^T \{F\} = \{Q\}$$

*Eq. [4]*

Hence, the only coupling between the resulting N equations is in the right-hand side. That is the way in which the structure is forced determines the coupling between the NM in Eq. [4].

The excitation of these uncoupled equations is not the physical force F directly; it is the generalized force vector  $\{Q\} = [\varphi]^T\{F\}$ .

If the structure is excited with an array of sinusoidal forces all at the same frequency with amplitude distributions proportional to one of the mode shapes weighted by the mass matrix

$$\{F\} = \alpha[M][\varphi]$$

*Eq. [5]*

where  $\alpha$  is real coefficient.

This results in a Q with zero values for all elements but the one corresponding to the selected mode shape as shown in Eq. [6].

$$\{Q\} = \alpha[\varphi]^T[M][\varphi] = \{0 \dots \alpha \dots 0\}^T$$

*Eq. [6]*

Hence the purpose of PRM is to iteratively tune the distribution of applied forces until the Q is null for all but the mode shape sought.

This approach is harder than it thought because practically many parameters are unknown. Thus, starting from the concept of a single DOF mode response, the first tuning approaches has been come up with for us. A single DOF has the phase changes from  $0^\circ$  to  $180^\circ$  with a passage at  $+90^\circ$  at the resonance, with the imaginary part only significant in a small bandwidth of  $2\zeta_n\omega_n$  centred at the resonance frequency.

Back in the days, E. Balmes et al [2] and Hutin [1] put it up the classical FAM. This method tries to define a set of force  $\{F\}$  all at the same frequency to apply for exciting the response of a single DOF mode.

Approximate criteria have been already used to evaluate the quality of single DOF mode isolation. They are known as Phase Criterion (to determine the resonance) and Quality Criterion (to give a measure of the rejection of unwanted modes). The first one is based on the PI phase deviation between master force control (input) and response, on the other hand the second is used to define the MIF as the ratio of the quadrature energy to the total energy (its value is 1 for a perfect appropriation).

Putting into practice the MIF formulation, and assuming a linear relationship between response and input by the FRFs, a generalized eigenvalue problem is derived to determine force inputs  $\{F\}$  (eigenvectors) that minimize MIF (eigenvalues).

The downside of this approach has provided a good determination of FRFs. The optimal forces are sensitive to noise in measured FRF and non-linear behaviour; this have brought to have some troubles from the changing of each form and level of input.

LAD's Large Structures Laboratories has built its practical experience on the NM tuning in the recent years. The tuning is performed by the using of MNM routine inside of Testlab<sup>TM</sup> software package.



From PSM a list of mode to be tuned is worked out before. For each mode it is selected the best excitation configurations for tuning. They depend on the PSM results, it is a practical usage to pull a single DOF mode out several times from different excitation runs. As a rule of thumb all excitation runs with good values of MPC and MPD can be considered good for tuning. Generally, the tuning is ensured by this condition

$$\text{MPC} > 90\% \text{ and } \text{MPD} < 15^\circ$$

*Eq. [7]*

Next step is due to the definition of the master control and response respectively.

Recalling the proprieties of a generic single DOF mode, the response control is that one almost in quadrature with the master control at the estimated resonance frequency. This latter gives us the chance to select the response control thru FRF data set provided by PSM results.

In MNM, FRF data set is usually downloaded in basis on the selected excitation run.

The choice of master control is mainly bound to expected mode shape. When more than two shakers are intending to use, the master control choice is very hard to do. But the master control for single mode is one of driving point applicants having the highest value of the mode participation (MP) parameter (the best one is very close to 100%).

Once the master control has been established, the remaining driving points work with amplitude ratio than the master level provided by FAM.

The target of the master force level has been changed properly during the testing. Sometimes it has been requested more force for nonlinearity compensations other times less force for instability tuning. The tuning method has been handled either manually or automatically. By experience the automatic tuning must be always guided by manual tuning before. Only after being sure to move around an uncoupled frequency mode, then it is possible to switch on the automatic approach. In some case, more than one iteration could be necessary to have the convergence. In both of cases, they have been established some thresholds on the PI and min MIF and then the shaker frequency is iteratively modified up to get 'tuned'. Experimentally speaking good tunings are obtained with:

$$\text{PI} \leq 90^\circ \pm 2^\circ \text{ and } \text{min MIF} \geq 0.99$$

*Eq. [8]*

As a usual, the A/C modes at low frequency can be tuned with one or two shakers working together. Besides at high frequency, more than two shakers could be needed.

The rigid body modes are generally not well sought with PRM.

When the NM is properly tuned it is possible the determination of the generalized parameters ( $\omega_j$ ,  $\zeta_j$ ,  $\mu_j$ ,  $\phi_j$ ). CPM, FQM and EDM are basically used by Leonardo for these purposes.

One of the advantages of MNM is the linearity check of modes in function of applied force. This is accomplished by conducting a series of force appropriations, each one with a different global force level. A plot of the resulting natural frequency-vs-force quickly identifies 'soft' or 'hard' nonlinear response.

Just to summary all GRT methodologies applied in LAD Large Structures Laboratories, in Figure 15 it is reported an overview of them by a logic workflow.

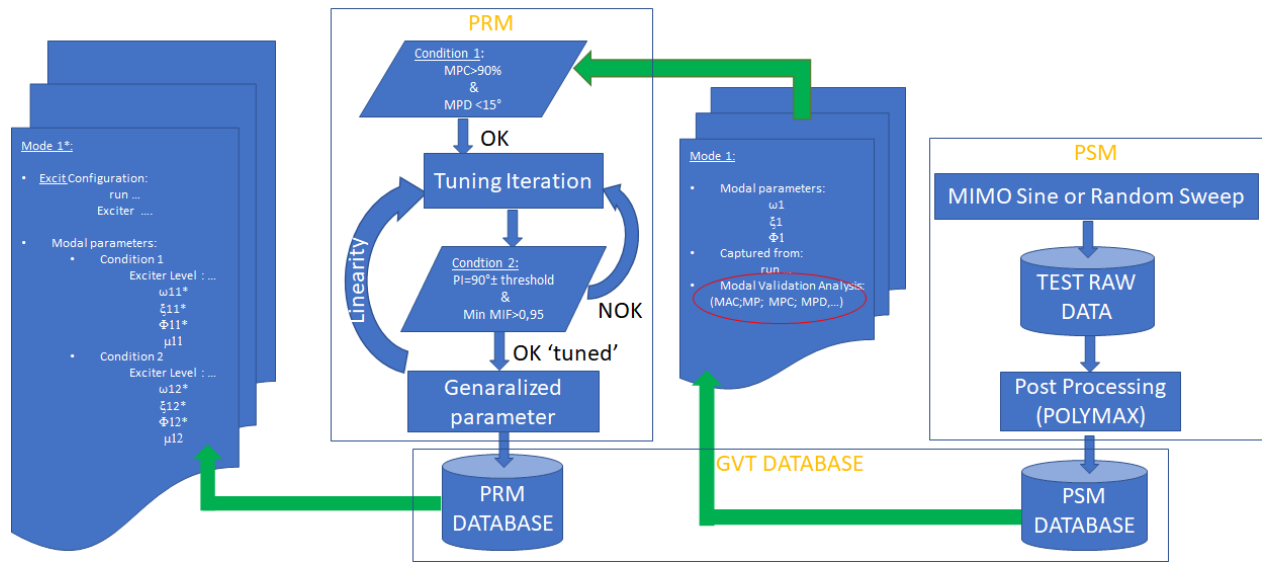


Figure 15 – Overview of Leonardo's GRT methods

## 6 GRT RESULTS

The GRT database has been obtained from various excitation runs with a total number of 87 tuned modes into the frequency range 0 to 50 Hz.

All rigid body modes have been identified, resulting well separated from the first normal modes.

In IWT configuration, the tests have been focused on the IWT modal identification and wing mode alterations. Only the IWT structure with relevant tab have been excited along Z direction.

In AMW configuration, the tests have been focused on the AMW modal identification and wing mode alterations. Only the AMW structure with relevant tab have been excited along Y and Z direction.

For each measured mode, the following data have been provided to LAD Aeroelastic specialists:

- mode shape  $\varphi$ ,
- natural frequency  $\omega$ , damping ratio  $\xi$  and generalized mass  $\mu$ ,
- linearity-plot.

The following figures show two examples of mode shape and linearity-plot, one for IWT configuration and one for AMW configuration.

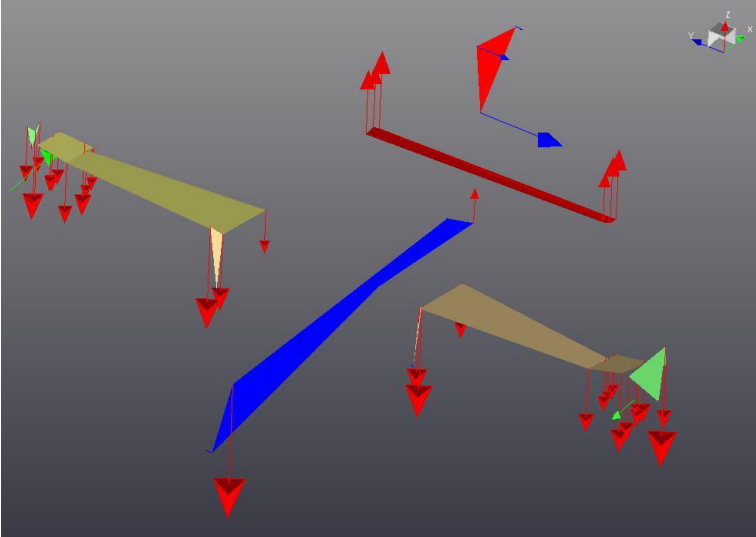


Figure 16 – IWT modal shape

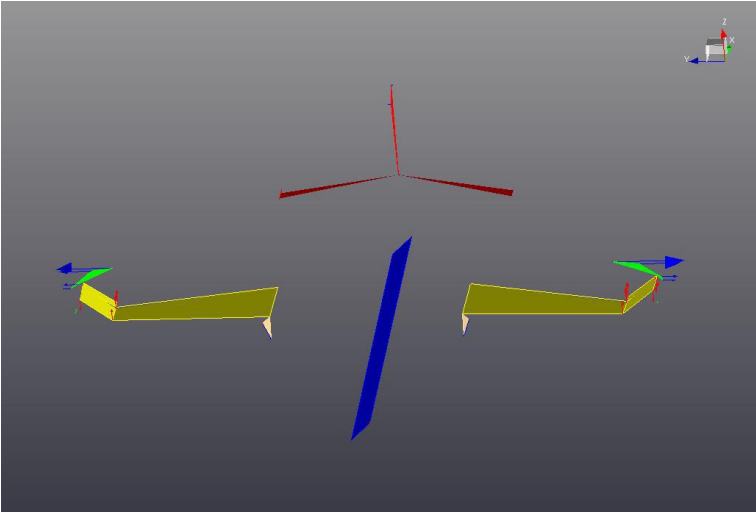


Figure 17 – AMW modal shape

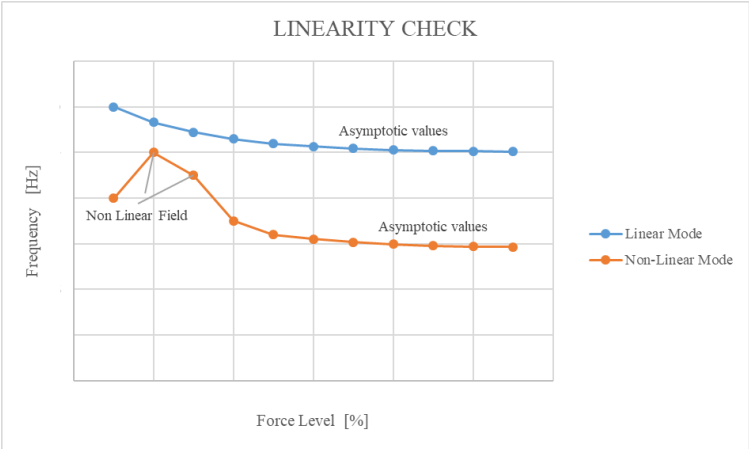


Figure 18 – Linearity plot

## 7 AEROELASTIC MODEL MATCHING AND APPLICABLE METHODS

Among all modes acquired by a GRT test of any platform, only the most reliable ones must be selected for the matching with the mathematical model.

The initial selection is obtained by the cross correlation of the modal shapes between all the selected measurements by means of the MAC calculation, in order to group the same modes that have been measured more than once. The MAC is an index that shows the correlation between modal shapes; value equal to 1 indicates that the compared modes have the same modal shape. If more experimental measurements are available for a mode, the modes with low MAC can be discarded.

$$MAC_{(i,j)} = \frac{|[\varphi_{GRT}]_i^T [W] [\varphi_{GRT}]_j|^2}{([\varphi_{GRT}]_i^T [W] [\varphi_{GRT}]_i)([\varphi_{GRT}]_j^T [W] [\varphi_{GRT}]_j)}$$

Eq. [9]

$[\varphi_{GRT}]$  represents the matrix of the measured modes; each mode- $i$  is compared with the mode- $j$  (with  $i$  and  $j$  from 1 to all measured modes). Values  $\geq 0.8$  indicate that the modal shapes can be considered matched from dynamic point of view; differences can be generally due either to the applied force levels that, when too high, can cause small oscillation of other parts of the A/C influencing the MAC calculation, or to some structural non-linearity.

Just as example of an asymmetry, the following Figure 19 shows the comparison of the same experimental modal shape acquired with different excitation force levels; the arrows represent the displacements measured by each pick-up. As it can be seen, the modal shapes differ mainly only on the displacements of inner wing trailing edges accelerometers, that are symmetric between RH and LH on the red picture. This small mismatching affects the MAC calculation that is about 0.56.

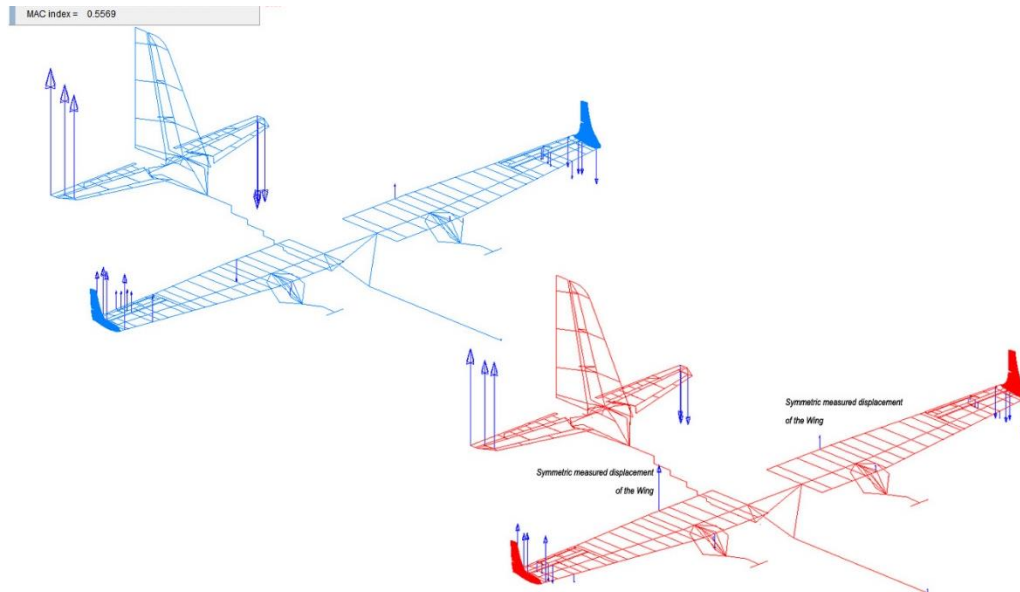


Figure 19 – Experimental Modal Shapes Comparison

In case that a local structural asymmetry is shown by experimental modes, which cannot be replicated by the model since defined symmetric between the right and left sides, the MAC between experimental and theoretical data can be improved by means of the weighing matrix  $[W]$  of Eq. [9]. Initially, all  $W$  elements (corresponding to the number of used accelerometers for each mode) are equal to 1, but in case that some accelerometer would be excluded from the MAC calculation, the relevant  $W$  can be put to 0.

Apart from the structural asymmetry of the A/C, another factor that can influence the MAC is the number of accelerometers used for GRT. The best solution should be the installation of a great number of pick-ups able to detect all structural resonances with a good acquisition of the modal shapes.

Mode A	19	41	58	23	38	22	40	39	18	21	57	42	17
[Hz]	0.79	2.97	3.99	4.00	5.43	5.46	5.45	5.48	7.53	8.30	8.31	8.34	8.37
0.79	1.00	0.61	0.06	0.08	0.00	0.00	0.00	0.00	0.00	0.01	0.00	0.00	0.00
2.97	0.61	1.00	0.02	0.02	0.00	0.00	0.00	0.00	0.02	0.06	0.10	0.10	0.08
3.99	0.06	0.02	1.00	0.97	0.00	0.01	0.00	0.07	0.06	0.16	0.00	0.01	0.01
4.00	0.08	0.02	0.97	1.00	0.01	0.01	0.00	0.05	0.04	0.14	0.00	0.00	0.00
5.43	0.00	0.00	0.00	0.01	1.00	0.99	0.37	0.26	0.26	0.16	0.00	0.00	0.00
5.46	0.00	0.00	0.01	0.01	0.99	1.00	0.36	0.29	0.28	0.15	0.00	0.00	0.00
5.45	0.00	0.00	0.00	0.00	0.37	0.36	1.00	0.25	0.11	0.03	0.00	0.00	0.00
5.48	0.00	0.00	0.07	0.05	0.26	0.29	0.25	1.00	0.01	0.00	0.00	0.00	0.01
7.53	0.00	0.02	0.06	0.04	0.26	0.28	0.11	0.01	1.00	0.31	0.11	0.11	0.12
8.30	0.01	0.06	0.16	0.14	0.16	0.15	0.03	0.00	0.31	1.00	0.63	0.65	0.67
8.31	0.00	0.10	0.00	0.00	0.00	0.00	0.00	0.00	0.11	0.63	1.00	0.98	0.98
8.34	0.00	0.10	0.01	0.00	0.00	0.00	0.00	0.00	0.11	0.65	0.98	1.00	0.99
8.37	0.00	0.08	0.01	0.00	0.00	0.00	0.00	0.01	0.12	0.67	0.98	0.99	1.00

Table 1 – AMW Measured Modes – MAC Correlation Table (Example of first modes)

As it can be seen as example in Table 1, more modes have been measured within a range of frequency.

Once that the experimental modes to be matched by the dynamic model are selected, the correlation of the modal shapes between the experimental and the theoretical ones is initially performed always by means of the MAC index calculation, substituting in Eq. [9] the  $[\varphi_{GRT}]_j$  with the  $j$ -theoretical modes calculated, obviously, on the same layout of the GRT accelerometers.

As said before, if some structural displacements can be considered negligible or not reliable, the relevant data can be neglected putting to 0 the relevant value of the matrix  $[W]$ .

The correlation of the frequencies should be obtained as consequence of the MAC matching. Commonly, the mass distribution is mainly derived from weighing of components and confirmed weighing the test article before the GRT. Some uncertainties could be derived from stiffness distributions, structural fittings and/or non-linearity (frictions or backlash).

The following Table 2 shows a summary of the modal matching between GRT and Model reporting the modal frequencies of GRT and Model, their differences in [Hz] and the MAC correlation (Figure 20). The names of modes are omitted and list is not complete due to company restrictions.

GRT [Hz]	Model [Hz]	Difference [Hz]	MAC
2.97	2.85	-0.12	1.0
4.00	3.88	-0.12	0.9
5.45	5.41	-0.04	0.8
7.53	7.39	-0.14	0.9
8.37	8.33	-0.04	1.0
9.46	9.12	-0.34	1.0
17.61	16.78	-0.83	0.9
24.80	23.90	-0.90	0.9

Table 2 – GRT and Model Matching (Example)

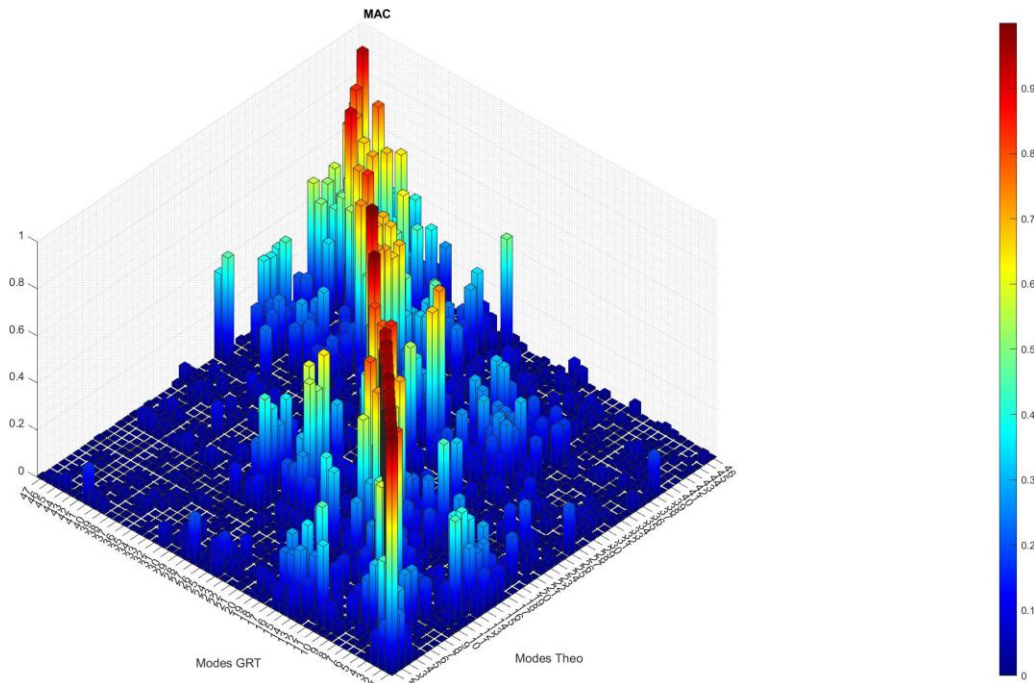


Figure 20 – MAC Correlation GRT Vs Theoretical Modes

Because of the FTB#1 aeroelastic model is derived from the C-27J one, already validated by GRT, the additional device installed on the wing tips does not have significant impact on modal shapes of the wing and tail planes and a good matching of relevant modes has been almost easily achieved.

Therefore, GRT have been focused mainly on peculiar modes of the new devices as bending, torsion and flap rotations, that have been measured and matched with the model; as example, the following Figure 21 and Figure 22 show the graphical matching achieved for the AMW bending symmetric and antisymmetric shapes (the red one is the GRT and the blue one the Nastran Model). The frequency of modes are not shown due to company restrictions.

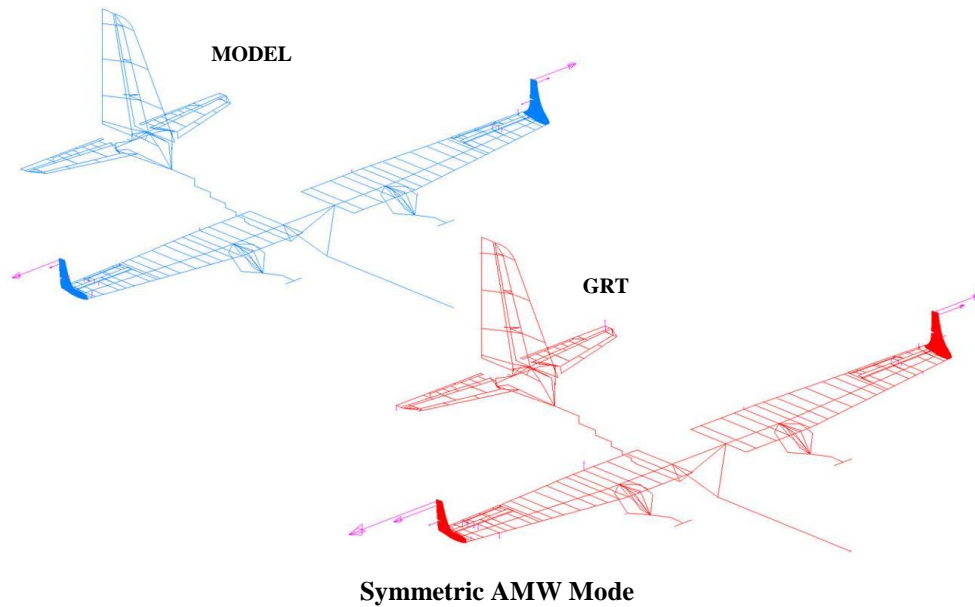


Figure 21 – Symmetric Modal Shape Comparison Model (Red) Vs GRT (Blue) – AMW Configuration (Accelerometer displacements)

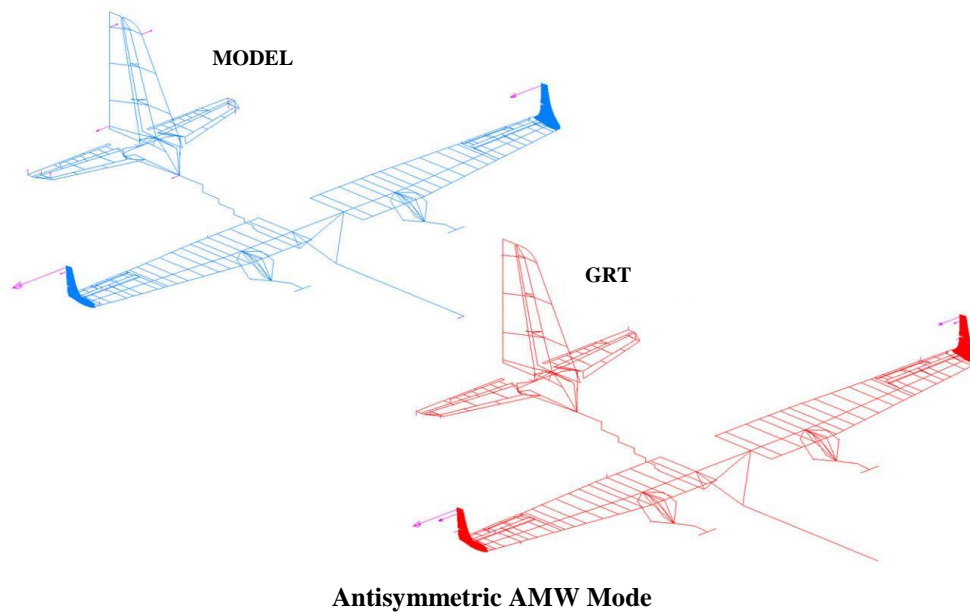


Figure 22 – Antisymmetric Modal Shape Comparison Model (Red) Vs GRT (Blue) – AMW Configuration (Accelerometer displacements)

The most important topic is the updating of the aeroelastic model to be validated on the basis of GRT measurements. There are different methods available to optimize an aeroelastic model: from the numerical optimizations as the Nastran design sensitivity SOL200 [1] to newer methodologies based, instead, on the so-called “Genetic” Algorithms (GA). All techniques allow to achieve a

good matching between the theoretical and the experimental frequencies and modal shapes measured during GRT campaign.

All optimization problem statements require an explicit description of the design objective, as well as bounds that define the region in which it may search. Concerning with numerical optimizer, you may ask for a design satisfying a minimum flexibility requirement, but without a proper weight budget, the design that the optimizer proposes may turn out to be unrealistic. Recommendations are needed also for the GA optimizer in the selection of the design parameters, the objective functions, constraints, etc., in order to achieve robust convergence without greatly increasing the processing time, or not reaching a premature convergence.

Therefore, a reasonable level of aeroelastic skill is required as concerns the models preparation and the assessment of the results and the proficiency in that discipline is mandatory.

Currently a Genetic process has been developed by LDO Aeroelastic Pool and it is supported by the software Esteco modeFRONTIER [2] (Figure 23) which manages, through the MATLAB scripts, the analyses performed by Nastran and the elaboration of the results (Figure 24), comparing the modal characteristics of each individual with the GRT experimental results. An important feature of modeFRONTIER is, in fact, the possibility to use different types of software of different manufacturers in a synergistic way.

These algorithms, inspired by the genetic evolution, are almost robust and able to explore with high efficiency the space of solutions, without focusing on specific area of input variables.

The genetic process enables to compose and manage all logical steps of an engineering design problem involving software platforms used in different disciplines, automates the simulation process and drives the integrated software platforms.

The approach to model matching involves treating it as a multi-objective optimization problem. This optimization utilizes a GA, employing a cyclical process in which various configurations of design variables (referred to as "individuals") are produced, assessed, and selected as genetic material for generating subsequent generations.

In any optimization procedure, it is essential that the operator specifies the design variables and establish objectives and constraints. The core of this process consists of a MATLAB routine designed to construct the models, launch analyses (for instance, using Nastran), interpret the outputs, and evaluate each individual. This evaluation supplies the optimizer with necessary data to generate a new population of data and to guide the optimization process effectively.

At the end of the optimization process the GA does not provide a single solution, but an optimal set of solutions (set of final individuals), where a design can be the best for one or more objectives of the problem, but on the other hand the worst for other objectives. These solutions are positioned on a "Pareto Front" (Figure 25) and the final one has to be selected by the aeroelastic specialist.



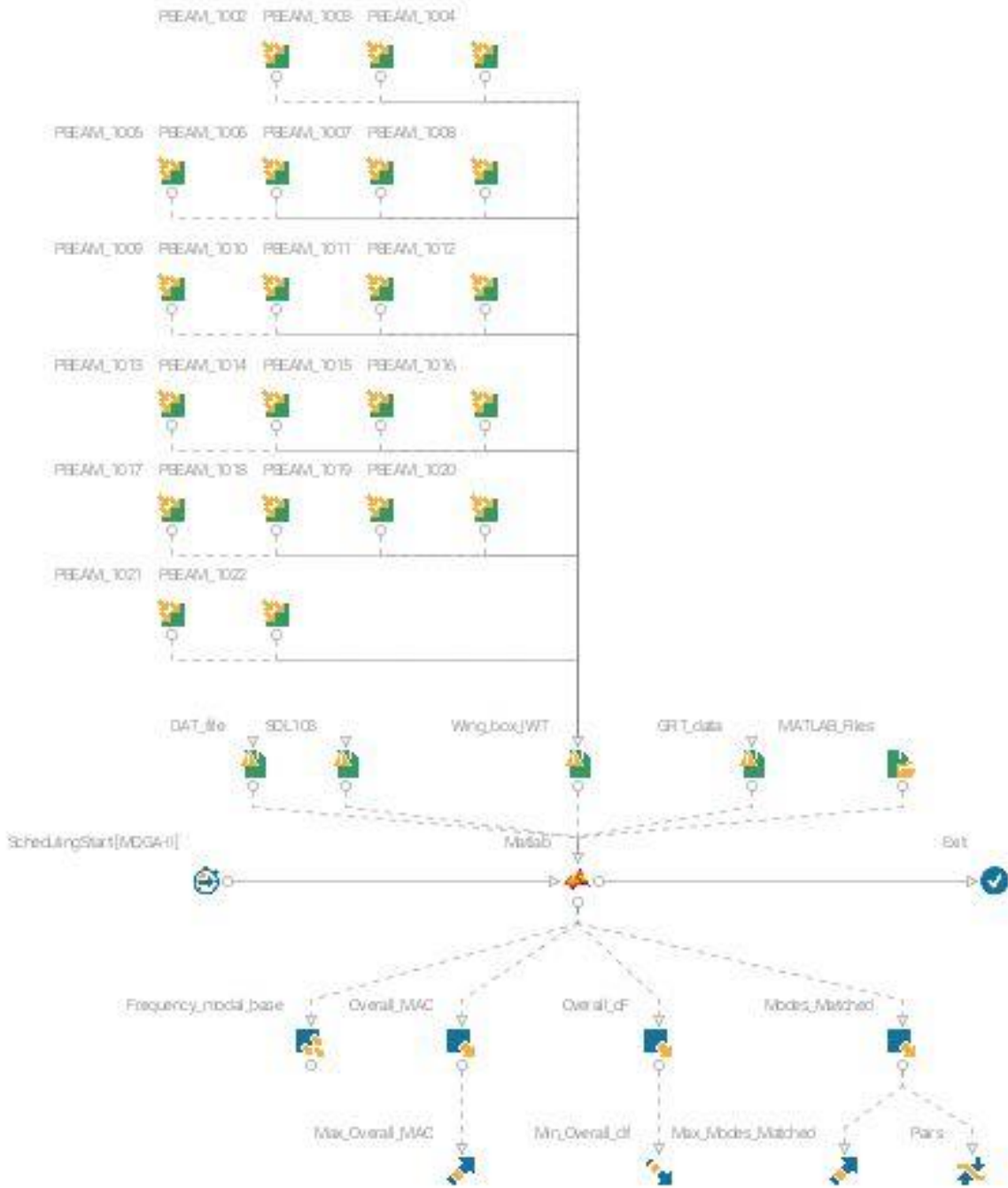


Figure 23 – Genetic Process Workflow

### EVOLUTION OF A GENETIC PROCESS

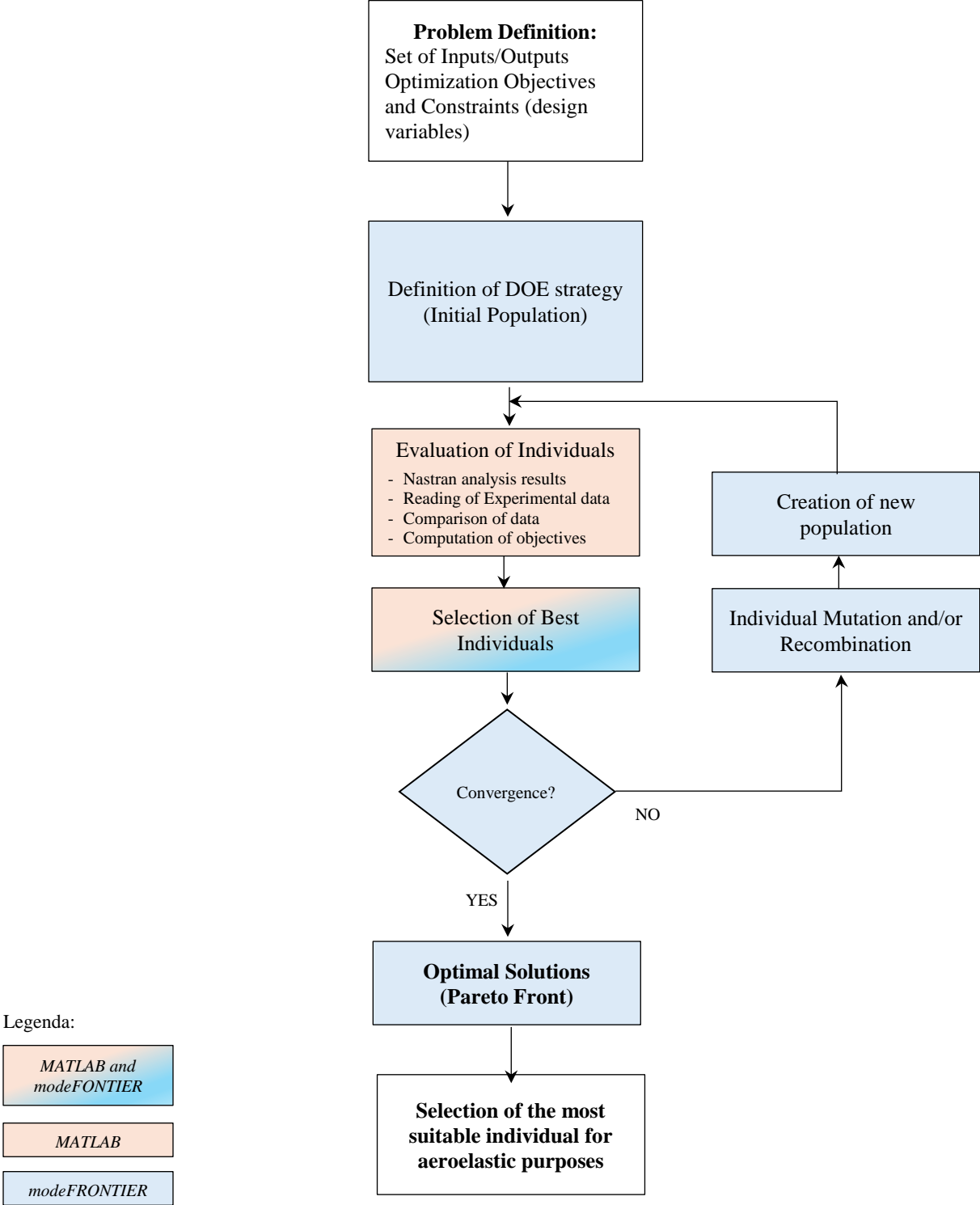
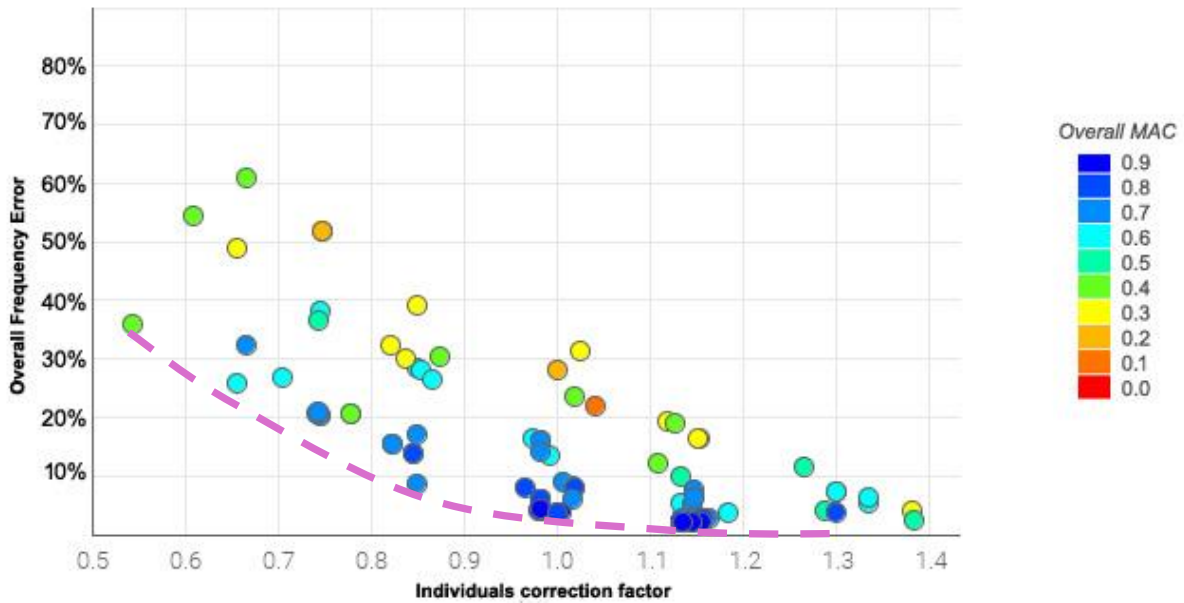


Figure 24 – Genetic Optimization Flow



Pareto Front

Figure 25 – Example of Pareto Front

As concerns the optimization of a dynamic model, design stiffness variables are previously identified as driver of the dynamic behavior of the model, in order to fit the experimental evidence. Potentially all element's parameters can be eligible to be part of this set (as the thickness of a panel, the Young/torsion module of a material, stiffness of the beams, etc.).

The mass distribution, that is mainly derived from weighing and replicated by lumped masses/inertia, are not considered subject to optimization because they are expected to well reproduce the inertial characteristics of the A/C and components.

Because the modal shapes are used for the generalization of the unsteady aerodynamic forces of aeroelastic analysis, the main goal for the dynamic model optimization is preferably a good matching of the modal shapes (MAC Eq. [9]) and then the resonance frequency.

Once that the  $i$ -th modal shape is well correlated and because of the aeroelastic analyses are based on the frequency domain using generalized stiffness and mass matrices, there are further tools developed by LDO Aeroelastic team that permits aeroelastic investigations correcting the generalized stiffness  $K_{GEN_i}$  aimed at the tuning of the  $f_i$  modal frequency as follows:

$$K_{GEN_i} = (2\pi f_i)^2 M_{GEN_i}$$

Eq. [10]

It is worth to point out that the Genetic optimization flow (Figure 24) can be also applicable for the optimization of the Nastran unsteady aerodynamic model that generally is based on the DLM [3].

An aerodynamic correction can deal, for example, the steady aerodynamic hinge moment coefficients of the primary control surfaces (since overestimated by DLM) based either on wind tunnel and/or CFD data, or on experimental measurements.

Looking, as example, at Figure 26 all lifting surfaces of the DLM model are assumed to lie parallel to the flow. Each of the interfering panels (shown with different colours) is divided into small trapezoidal lifting elements (“boxes”), such that the boxes are arranged in strips parallel to the free stream ( $V_\infty$ ) with surface edges and hinge lines that lie on box boundaries.

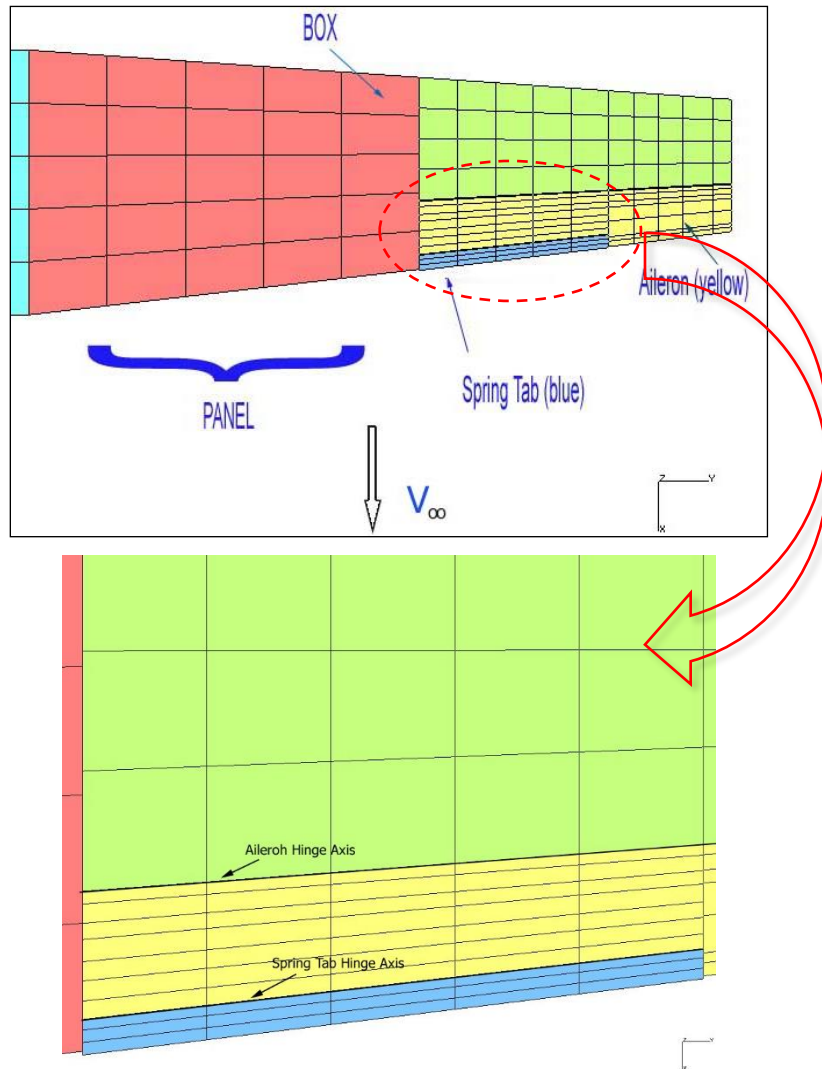


Figure 26 – Aileron/Tab DLM Aerodynamic Boxes

The correction factors matrix is named in Nastran [ $W_{kk}$ ] (or WTFACT), shown in Eq. [11], and it can be introduced into the aeroelastic solutions (SOL144, SOL145 and SOL146) via DMI entries:

$$[Q_{ii}] = [\varphi_{ai}]^T [G_{ka}]^T [W_{kk}] [Q_{kk}] [G_{ka}] [\varphi_{ai}]$$

Eq. [11]

Where:

$[Q_{ii}]$  – generalized aerodynamic matrix

$[Q_{kk}]$  – aerodynamic influence coefficients of each theoretical aerodynamic box

$[\varphi_{ai}]$  – matrix of *i-set* normal mode vectors in the physical a-set

$[W_{kk}]$  – matrix of correction factors to adjust each theoretical aerodynamic box

The goal of the DLM optimization could be the matching of the coefficients of the hinge aerodynamic moments  $Ch$ .

$$Ch_{\delta a} = b_0 + b_1\alpha + b_2\delta_a + b_3\delta_t \quad \text{Eq. [12]}$$

$$Ch_{\delta t} = c_0 + c_1\alpha + c_2\delta_a + c_3\delta_t \quad \text{Eq. [13]}$$

$b_0$  and  $b_1$  (as well as  $c_0$  and  $c_1$ ) are the aileron (tab) gradients respectively due to surface profile and wing angle of attack  $\alpha$ , while  $b_2$  and  $b_3$  (as well as  $c_2$  and  $c_3$ ) are directly dependent on control surface rotations  $\delta_a$  and  $\delta_t$  and can be calculated by means of partial derivative as:

$$b_2 = \frac{\partial Ch_{\delta a}}{\partial \delta_a} \quad b_3 = \frac{\partial Ch_{\delta a}}{\partial \delta_t} \quad \text{Eq. [14]}$$

$$c_2 = \frac{\partial Ch_{\delta t}}{\partial \delta_a} \quad c_3 = \frac{\partial Ch_{\delta t}}{\partial \delta_t} \quad \text{Eq. [15]}$$

These four gradients of Eq. [14] and Eq. [15] are provided, in general, by wind tunnel and/or CFD data, or by experimental measurements and are to be matched by the corrective process.

The tool of the Genetic process developed by LDO Aeroelasticity manages, through MATLAB, the Nastran steady aeroelastic analysis SOL144 that calculates the steady hinge moments of control surfaces and the elaboration of the results in MATLAB.

A first set of population is identified and iterations are repeated until one or more set of optimal solutions match the target values; the aeroelastic specialist selects the final set of corrective coefficients stored in the  $[W_{kk}]$  matrix.

## 8 CONCLUSIONS

In this paper there deals with all characteristic steps for the ground test campaign running, data post-processing and finally test data correlation with aeroelastic model used to provide the flight clearances and the related permit to fly tests aimed at reaching the TRL6 of the studied technologies on an innovative Green Regional Aircraft formulated by CS2 program and equipped with AMW and IWT.

Since GRT has to be performed before the first flight, it is always placed on the critical path of delivery process issued by Airworthiness Authorities.

The relevant GRTs were carried out in efficient way by a few number of shaker in the frequency in free-free configuration and the most relevant A/C elastic modes were extracted successfully thanks to the advanced methods described herein step-by-step.

The GRT results met to all test specifications and showed the maturity of LAD team, thus it is necessary to have always at hand technical approaches to make as shorten as possible the relevant timeline. A high correlation between various typologies of test excitations was achieved, confirming the accuracy of the experimental approaches.

The aeroelastic model matching is a specific issue strictly dependent on the nature of the models. Correlating mathematical modal behavior with experimental evidences is a critical task because of the many effects that a model has to represent, in some case also nonlinear.

Matching process is then necessary to ensure the reliability of the model and thereby its validation and it is conducted by comparing it to the most reliable experimental data, as described in this paper. Therefore, different optimization approaches have been developed by LAD Aeroelastic Pool, currently based on GA to manage the achievement of the optimization targets. Optimization process based on GA to update mathematical models (structural and aerodynamic models) has proven to increase their level of fidelity, confirming its strength to probe a vast design space efficiently and effectively.

The mentioned GA process has been applied to update the aeroelastic model of the FTB#1 A/C fitted on wing tips with innovative morphing devices developed within the CS2 program, in order to perform all needed aeroelastic investigation aimed at the achievement of the first permit to fly.

The aeroelastic model in configuration FTB#1+IWT, optimized and validated on the basis of GRT data, has been used to provide the clearances of first flight that was carried out in 12/02/2024 achieving the TRL6 of the studied technologies.

**REFERENCES**

- [1] C. Hutin- (2000) *Modal Analysis using Appropriated Excitation Techniques* Sound and Vibration 2000
- [2] E. Balmes, C. Chapelier, P. Lubrina, P. Fargette (1995). *An evaluation of modal testing results based on the force appropriation method*. Proceedings of IMAC 1995.
- [3] SIEMENS - Nastran Design Sensitivity and Optimization User's Guide (SOL 200)
- [4] "modeFRONTIER Simulation automation and design optimization". Retrieved 2023-09-13. [engineering.esteco.com](http://engineering.esteco.com)
- [5] SIEMENS - Nastran Aeroelastic Analysis User's Guide

**COPYRIGHT STATEMENT**

The authors confirm that they, and/or their company or organisation, hold copyright on all of the original material included in this paper. The authors also confirm that they have obtained permission from the copyright holder of any third-party material included in this paper to publish it as part of their paper. The authors confirm that they give permission, or have obtained permission from the copyright holder of this paper, for the publication and public distribution of this paper as part of the IFASD 2024 proceedings or as individual off-prints from the proceedings.